# Highly Sensitive Temperature Sensing Using the Silicon Vacancy in Silicon Carbide by Simultaneously Resonated Optically Detected Magnetic Resonance

Yuichi Yamazaki[1,*], Yuta Masuyama[1], Kazutoshi Kojima[2], and Takeshi Ohshima[1]

[1]*National Institutes for Quantum Science and Technology, Quantum Materials and Applications Research Center, Takasaki, Gunma 370-1292, Japan*

[2]*National Institute of Advanced Industrial Science and Technology, Advanced Power Electronics Research Center, Tsukuba, Ibaraki 305-8568, Japan*

Quantum sensors using silicon vacancy ($V_{Si}$) in silicon carbide (SiC) are expected to be capable of directly measuring inside SiC devices. It is a serious problem that we have to employ the excited state (ES) of $V_{Si}$ with very low temperature sensitivity for quantum sensing due to there being no temperature sensitivity for the ground state (GS). Here, we propose a temperature measurement protocol, simultaneously resonated optically detected magnetic resonance (SRODMR), based on the modulation of the GS ODMR response resulting from simultaneous resonance of both GS and ES. This protocol diverts part of the GS ODMR contrast to temperature measurement, and in principle, temperature can be measured at an equivalent signal intensity to that of GS ODMR. SRODMR improves signal intensity by 1 order of magnitude compared with the conventional method (ES ODMR), leading to temperature measurements with a smaller error.

Quantum sensing using optically addressable defects in wide-band-gap materials, i.e., spin defects, is a promising technique because it can measure magnetic and electric fields and temperature with highly sensitive and high spatial resolution. A negatively charged nitrogen-vacancy composite defect (N-$V^-$ center) in diamond [1] is the spin defect that shows the highest sensor performance at this time and has been studied in a wide range of applications [2–6]. In silicon carbide (SiC), several spin defects acting as quantum sensors have been found, such as a negatively charged silicon vacancy ($V_{Si}^-$) [7–9], a neutral divacancy ($V_C V_{Si}$, $VV^0$) [10,11], and a negatively charged pair of $V_{Si}$ and nitrogen atom (N) on an adjacent carbon (C) site ($N_C V_{Si}^-$) [12,13]. For $V_{Si}^-$, magnetic field and temperature sensing have already been demonstrated [7,14,15]. SiC is well known as a material for power semiconductors [16], and the latest commercial products have blocking voltage of more than 1000 V. Higher-blocking-voltage power devices are expected to apply to application fields such as a battery management system of electric vehicles and power converters for high-voltage direct current power transmission systems, and contribute to further system miniaturization and energy savings. To develop devices, detailed data of internal states in SiC devices in operation should be helpful because the data enable us to carry out precise simulation and design more sophisticated

device layout. In this regard, a $V_{Si}$-based quantum sensor operating at and above room temperature is a unique tool to observe the inside of SiC devices directly with highly sensitive and high spatial resolution. We have proved that optically detected magnetic resonance (ODMR), which is a measurement principle of quantum sensors, is possible even under current flow [17]. This is an important step for realizing direct quantum sensing in a device in operation. As electrically detected magnetic resonance [18–20] can detect magnetic fields using device current instead of optical access, it is suitable for direct measurements. However, temperature detection has not been demonstrated yet.

In general, the ground state (GS) of spin defects is employed for ODMR because GS ODMR gives rise to a larger ODMR contrast (higher sensitivity) than that of the excited state (ES). For thermometry, a $V_{Si}$-based quantum sensor has the disadvantage that GS ODMR shows no temperature sensitivity [14], which forces us to select ES ODMR for temperature sensing, at much lower contrast [21]. This makes temperature measurement very difficult. Although simultaneous measurement of magnetic field and temperature is desirable from the viewpoint of time efficiency, temperature measurement is currently an obstacle. Therefore, highly sensitive temperature measurement methods are strongly required.

In this work, we propose a temperature sensing method, simultaneously resonated ODMR (SRODMR), which can measure temperature with higher signal intensity than the conventional ES ODMR. The method is based on the

*yamazaki.yuichi@qst.go.jp

phenomenon that the GS ODMR contrast is modified under simultaneous resonance of GS and ES. It enables us to measure temperature with, in principle, leveraging of the equivalent sensitivity of GS ODMR. We demonstrate that SRODMR improves signal intensity by 1 order of magnitude compared with ES ODMR, which leads to higher-precision temperature measurements.

Samples used in this study are a 5.6-$\mu$m-thick $p$-type SiC epitaxial layer with a doping concentration of $1.5 \times 10^{16}$ cm$^{-3}$, grown on $n$-type SiC substrate. Dot patterns consisting of $V_{Si}$ ensemble ($5 \times 5$ $\mu$m$^2$ in size, 30 $\mu$m in pitch) were created in the samples by particle beam writing [22] using a focused ($\phi \sim 1$ $\mu$m) He beam. The ion energy and fluence were 0.5 MeV and $3 \times 10^5$ He$^+$/spot, respectively. The depth of $V_{Si}^-$ was estimated to be approximately 1 $\mu$m by stopping and range of ions in matter simulation [23]. Samples were then annealed at 600 °C to improve the optical and spin properties of $V_{Si}^-$ [24]. ODMR measurements were performed on one of the dot patterns ($V_{Si}^-$ ensemble) by a home-built confocal microscope. A 785-nm laser was chosen to maximize excitation efficiency of $V_{Si}^-$ [25]. The laser power was set to 0.5 mW (spot size $\sim 4$ $\mu$m) for all experiments. For ODMR measurements, to resonate GS (30–110 MHz) and ES (200–500 MHz) simultaneously, a radio frequency (rf) field was applied to a sample through a copper wire followed by combining two rf's from two signal generators (SG1 and SG2) and amplification as shown in Fig. 1(a). The rf for GS was amplitude modulated to detect a signal using our software lock-in system. A 900-nm long-pass filter was used to remove background luminescence. The sample was heated to around 400 K in air by a resistive heater.

Firstly, we explain the evolution of GS ODMR spectra on which SRODMR is based. Figures 1(b) and 1(c) show the GS ODMR spectra measured on and off ES resonance, respectively. For on-resonance, ODMR contrast

decreased with increasing rf power for ES (RF$_{ES}$). On the other hand, no significant change in contrast was observed for off-resonance. The results indicate that the change of contrast in GS ODMR is expected to occur only at simultaneous resonance of GS and ES. Hence, the following temperature measurement protocol, SRODMR, is proposed. We observe the changing ODMR contrast by sweeping the rf frequency for ES while keeping GS on-resonance. The rf for ES leading to changes of GS ODMR contrast signifies the rf resonance of ES. We can now determine the temperature from the frequency: The signal intensity of SRODMR should correspond to the decrease in GS ODMR contrast, and therefore its sign should be negative. Since this protocol diverts part of the GS ODMR contrast to the signal intensity of SRODMR, in principle, SRODMR can measure temperature leveraging the equivalent signal intensity of the ground state if 100% diversion is realized by higher RF$_{ES}$.

We verified the proposed protocol as follows. Figure 2 shows a comparison of SRODMR and ES ODMR spectra. The SRODMR signal showed a negative sign as expected, and a positive sign for ES ODMR due to our software lock-in system. SRODMR improved signal intensity by 1 order of magnitude compared with ES ODMR upon RF$_{ES}$ of 40 dBm. In addition, the signal was observable even at smaller RF$_{ES}$ for SRODMR. All spectra showed a change in amplitude at around 400 MHz, which corresponds with the resonance frequency for ES at room temperature [14,21]. A slight shift of resonance frequency for SRODMR upon RF$_{ES} = 30$–40 dBm was attributed to a slight temperature rise due to higher RF$_{ES}$ [26]. On the other hand, there is no shift in resonance frequency due to temperature changes caused by RF$_{GS}$ because RF$_{GS}$ is considerably less power than RF$_{ES}$ during SRODMR measurements (data not shown). The intensity change observed around 380 MHz was presumed to be originated not from $V_{Si}$ but from the measurement system because no
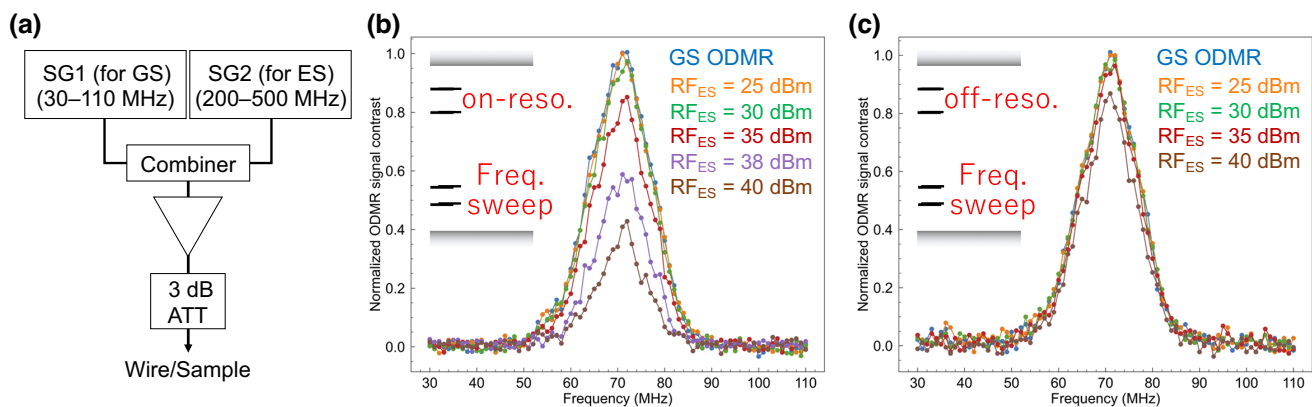


FIG. 1.   (a) An rf-based setup for SRODMR. Evolution of GS ODMR spectra (b) under on-resonance in ES (410 MHz) and (c) under off-resonance in ES (300 MHz). RF$_{GS}$ is amplitude modulated. For on-resonance, increasing RF$_{ES}$ leads to a decrease of GS ODMR contrast. No significant change occurs for off-resonance.
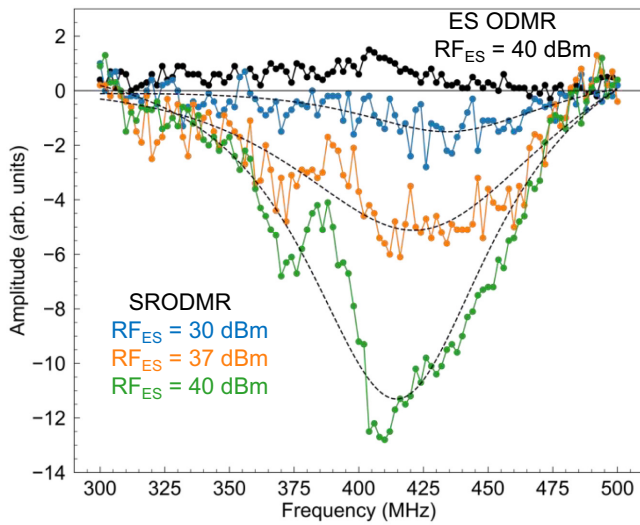
FIG. 2. Comparison of SRODMR [$RF_{GS}$ (70 MHz) modulated] and ES ODMR ($RF_{ES}$ modulated) spectra. The dotted lines show the result of fitting by Lorenz function for SRODMR, where the central frequencies are 434 MHz ($RF_{ES} = 30$ dBm), 421 MHz (37 dBm), and 415 MHz (40 dBm).

of GS ODMR contrast is observable as shown in Fig 1(c). For on-resonance [Fig. 4(d)], the electrons with a large spin polarization are photoexcited to ES and then are resonated once again by $RF_{ES}$. Since the amount of rf absorption is proportional to the spin polarization, a large change in polarization can be obtained even for very short lifetime in ES compared with single-resonance ES ODMR [Fig. 4(c)]. The resultant GS ODMR contrast will be smaller due to a smaller spin polarization. As a result, we can observe this behavior shown in Fig. 1(b). Increasing GS ODMR contrast by larger $RF_{GS}$ results in a larger SRODMR signal intensity at the same $RF_{ES}$. Thus, the $RF_{GS}$ dependence of SRODMR signal intensity is similar to that of GS ODMR. With increasing $RF_{ES}$, although spin polarization is the same for each $RF_{GS}$, the change in polarization increases. This makes the increase rate of SRODMR signal intensity large. As described above, SRODMR signal intensity can be explained by the change of spin polarization modulated by both $RF_{GS}$ and $RF_{ES}$. The reason for a large signal intensity compared with ES ODMR is that SRODMR causes the resonance in ES under a large spin polarization generated by the resonance in GS. In contrast,

temperature dependence was confirmed for the intensity change on temperature measurements described below. Significant improvement in signal intensity resulted in a shorting of measurement time by more than 1 order of magnitude as shown in Figs. 3(a) and 3(b). These results clearly show that SRODMR is capable of measuring temperature with higher sensitivity owing to higher signal intensity as well as shorter measurement time [27]. In addition, we confirmed the similar evolutions of GS ODMR spectra under external magnetic fields ($B//c$). This indicates that SRODMR is also applicable to simultaneous measurement of magnetic field and temperature.

Here, we discuss the mechanism of SRODMR using the experimental results and spin polarization processes for GS and ES. The $RF_{GS}$ and $RF_{ES}$ dependence of SRODMR signal intensity was investigated as shown in Fig. 4(a). The signal intensity increased with increasing $RF_{GS}$ at each $RF_{ES}$. The larger the $RF_{ES}$, the greater the rate of increase in amplitude is observed. This experimental result can be attributed to following mechanism [Figs. 4(b)–4(d)]. Initially, there is almost no spin polarization among each spin sublevel in GS due to thermal equilibrium. Increase of $RF_{GS}$ results in increasing spin polarization in GS. This leads to $RF_{GS}$ dependence as shown in the inset of Fig. 4(a). Similar rf power dependence of GS ODMR contrast has been reported [28]. In the same manner, spin polarization in ES increases with increasing $RF_{ES}$ although the effect in ES is smaller than that in GS due to very short lifetime as short as 6 ns in ES [25]. As the spin polarization process for SRODMR with off-resonance in ES is equivalent to that for GS ODMR [Fig. 4(b)], no significant change
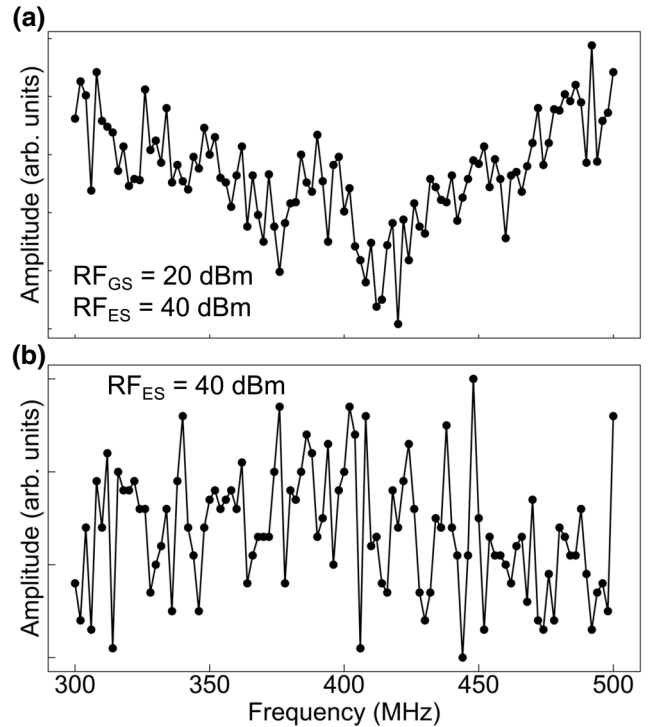


FIG. 3. Comparison of measurement time. (a) SRODMR spectrum for duration of 30 min and (b) ES ODMR spectrum for duration of 5 h. SRODMR signal can be detected for 30 min. In contrast, ES ODMR signal is not observed even for a 5-h measurement. These results indicate that SRODMR can also shorten the measurement time, resulting in higher sensitivity.
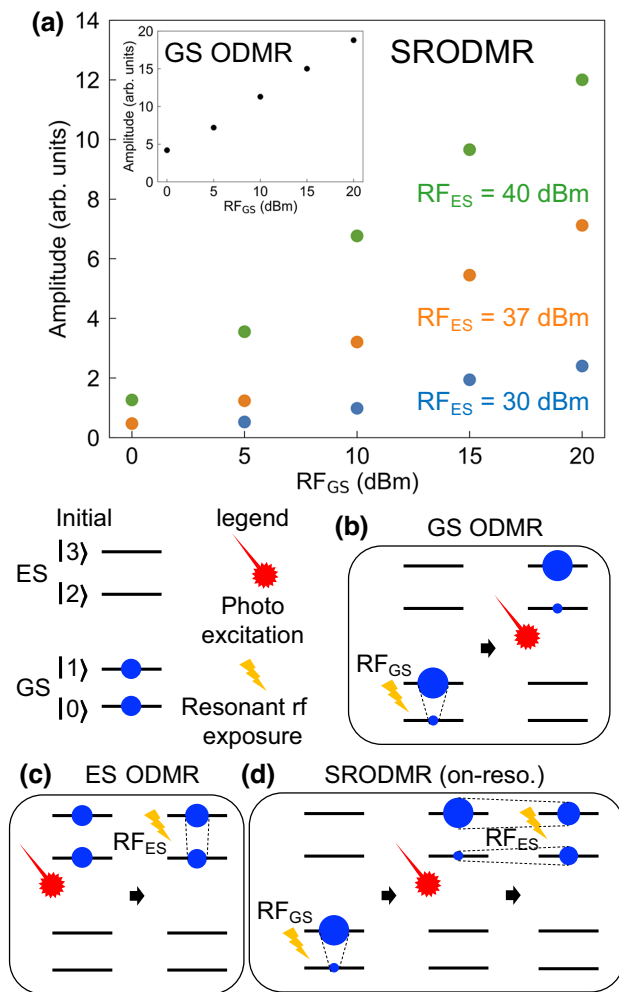
FIG. 4. (a) $RF_{GS}$ and $RF_{ES}$ dependence of SRODMR signal intensity. Inset shows $RF_{GS}$ dependence of GS ODMR signal intensity. Spin polarization processes for (b) GS ODMR, (c) ES ODMR, and (d) SRODMR with on-resonance in ES. The size of blue circles qualitatively indicates spin population. Unlike conventional ODMR, two resonances occur in both GS and ES for SRODMR, resulting in a large change in spin polarization. This leads to a larger signal intensity compared with ES ODMR.
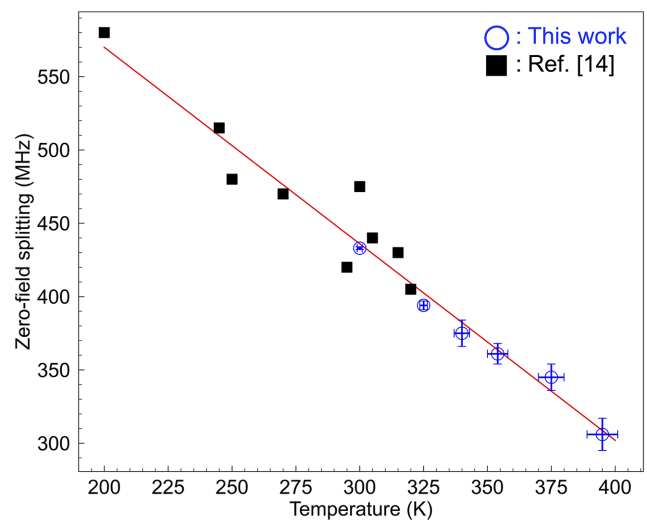


FIG. 5. Temperature measurement by SRODMR. Blue circles and black solid squares are data obtained in this work and a previous study [11], respectively. Red line represents the result of linear fitting, conducting a thermal shift of 1.3 MHz/K. To account for temperature rise caused by rf exposure, a resonance frequency for $RF_{ES} = 30$ dBm is plotted at 300 K.

for ES ODMR, only a small amount of polarization is realized even with high $RF_{ES}$, resulting in a very small ODMR contrast.

Finally, temperature measurement using SRODMR is demonstrated. The results are shown in Fig. 5. A similar temperature dependence of resonance frequency as in a previous study [14] was obtained, corroborating that SRODMR is a viable temperature measurement technique. The thermal shift was calculated to be 1.3 MHz/K in this temperature range, a value that is smaller than that obtained in the previous study. This may be caused by a nonlinear thermal shift observed over a wide temperature range, especially low temperature, for other spin defects [29–31]. The maximum temperature we measured in this demonstration was 395 K, a limitation due to our setup hardware. It does not constitute an intrinsic limit of the material or method, as proven by significant residual signal intensity at 395 K.

In summary, we propose a temperature sensing protocol, SRODMR, for a $V_{Si}$-based quantum sensor. The protocol is based on the phenomenon that simultaneous resonance of GS and ES leads to a decrease of GS ODMR contrast. SRODMR not only improves signal intensity by 1 order of magnitude, but also contributes to much shorter measurement time. We succeed in measuring temperature up to 395 K (122 °C). This demonstrates the effectiveness of SRODMR as a highly sensitive temperature measurement method. Recently, improvement of GS ODMR contrast has been reported [28,32]. Since the improvement is directly related to the increase in SRODMR signal intensity, further sensitivity improvements in temperature measurements can be expected by combining the reported findings with SRODMR. We do not evaluate sensitivity at this time, because we focus on dynamic range for application as a direct *in situ* measurement inside operating SiC devices. However, it is estimated that sensitivity would also be improved by using SRODMR due to both higher signal intensity and much shorter measurement time. Some spin defects, such as $V_{Si}$ in SiC, may cause ES to have a larger change in resonant frequency with respect to temperature, pressure, and electric field measurements compared with GS. In such cases, SRODMR must be useful because both the large signal intensity and a large shift

lead to highly sensitive quantum sensing. From this perspective, SRODMR is a promising measurement protocol that expands the possibilities of quantum sensing.

[1] A. Gruber, A. Dräbenstedt, C. Tietz, L. Fleury, J. Wrachtrup, and C. von Borczyskowski, Scanning confocal optical microscopy and magnetic resonance on single defect centers, Science **276**, 2012 (1997).

[2] G. Kucsko, P. C. Maurer, N. Y. Yao, M. Kubo, H. J. Noh, P. K. Lo, H. Park, and M. D. Lukin, Nanometre-scale thermometry in a living cell, Nature **500**, 54 (2013).

[3] T. Iwasaki, W. Naruki, K. Tahara, T. Makino, H. Kato, M. Ogura, D. Takeuchi, S. Yamasaki, and M. Hatano, Direct nanoscale sensing of the internal electric field in operating semiconductor devices using single electron spins, ACS Nano **11**, 1238 (2017).

[4] J.-P. Tetienne, N. Dontschuk, D. A. Broadway, A. Stacey, D. A. Simpson, and L. C. L. Hollenberg, Quantum imaging of current flow in graphene, Sci. Adv. **3**, e1602429 (2017).

[5] F. Casola, T. van der Sar, and A. Yacoby, Probing condensed matter physics with magnetometry based on nitrogen-vacancy centres in diamond, Nat. Rev. Mater. **3**, 17088 (2018).

[6] S. Sotoma, H. Okita, S. Chuma, and Y. Harada, Quantum nanodiamonds for sensing of biological quantities: Angle, temperature, and thermal conductivity, Biophys Physicobiol. **19**, e190034 (2022).

[7] M. Widmann, S.-Y. Lee, T. Rendler, N. T. Son, H. Fedder, S. Paik, L.-P. Yang, N. Zhao, S. Yang, I. Booker, A. Denisenko, M. Jamali, S. A. Momenzadeh, I. Gerhardt, T. Ohshima, A. Gali, E. Janzén, and J. Wrachtrup, Coherent control of single spins in silicon carbide at room temperature, Nat. Mater. **14**, 164 (2015).

[8] F. Fuchs, B. Stender, M. Trupke, D. Simin, J. Pflaum, V. Dyakonov, and G. V. Astakhov, Engineering near-infrared single-photon emitters with optically active spins in ultrapure silicon carbide, Nat. Commun. **6**, 7578 (2015).

[9] T. Ohshima, T. Satoh, H. Kraus, G. V. Astakhov, V. Dyakonov, and P. G. Baranov, Creation of silicon vacancy in silicon carbide by proton beam writing toward quantum sensing applications, J. Phys. D: Appl. Phys. **51**, 333002 (2018).

[10] D. J. Christle, A. L. Falk, P. Andrich, P. V. Klimov, J. Ul Hassan, N. T. Son, E. Janzén, T. Ohshima, and D. D. Awschalom, Isolated electron spins in silicon carbide with millisecond coherence times, Nat. Mater. **14**, 160 (2015).

[11] C. F. de las Casas, D. J. Christle, J. U. Hassan, T. Ohshima, N. T. Son, and D. D. Awschalom, Stark tuning and electrical charge state control of single divacancies in silicon carbide, Appl. Phys. Lett. **111**, 262403 (2017).

[12] J.-F. Wang, F.-F. Yan, Q. Li, Z.-H. Liu, H. Liu, G.-P. Guo, L.-P. Guo, X. Zhou, J.-M. Cui, J. Wang, Z.-Q. Zhou, X.-Y. Xu, J.-S. Xu, C.-F. Li, and G.-C. Guo, Coherent Control of Nitrogen-Vacancy Center Spins in Silicon Carbide at Room Temperature, Phys. Rev. Lett. **124**, 223601 (2020).

[13] Z. Mu, S. A. Zargaleh, H. J. von Bardeleben, J. E. Fröch, M. Nonahal, H. Cai, X. Yang, J. Yang, X. Li, I. Aharonovich, and W. Gao, Coherent manipulation with resonant excitation and single emitter creation of nitrogen vacancy centers in 4H silicon carbide, Nano Lett. **20**, 6142 (2020).

[14] A. N. Anisimov, D. Simin, V. A. Soltamov, S. P. Lebedev, P. G. Baranov, G. V. Astakhov, and V. Dyakonov, Optical thermometry based on level anticrossing in silicon carbide, Sci. Rep. **6**, 33301 (2016).

[15] T. M. Hoang, H. Ishiwata, Y. Masuyama, Y. Yamazaki, K. Kojima, S.-Y. Lee, T. Ohshima, T. Iwasaki, D. Hisamoto, and M. Hatano, Thermometric quantum sensor using excited state of silicon vacancy centers in 4H-SiC devices, Appl. Phys. Lett. **118**, 044001 (2021).

[16] X. She, A. Q. Huang, Ó Lucía, and B. Ozpineci, Review of silicon carbide power devices and their applications, IEEE Trans. Ind. Electron. **64**, 8193 (2017).

[17] Y. Yamazaki, Y. Chiba, S.-i Sato, T. Makino, N. Yamada, T. Satoh, K. Kojima, Y. Hijikata, H. Tsuchida, N. Hoshino, S.-Y. Lee, and T. Ohshima, Carrier dynamics of silicon vacancies of SiC under simultaneous optically and electrically excitations, Appl. Phys. Lett. **118**, 021106 (2021).

[18] C. J. Cochrane, P. M. Lenahan, and A. J. Lelis, An electrically detected magnetic resonance study of performance limiting defects in SiC metal oxide semiconductor field effect transistors, J. Appl. Phys. **109**, 014506 (2011).

[19] C. J. Cochrane, J. Blacksberg, M. A. Anders, and P. M. Lenahan, Vectorized magnetometer for space applications using electrical readout of atomic scale defects in silicon carbide, Sci. Rep. **6**, 37077 (2016).

[20] Y. Abe, A. Chaen, M. Sometani, S. Harada, Y. Yamazaki, T. Ohshima, and T. Umeda, Electrical detection of TV2a-type silicon vacancy spin defect in 4H-SiC MOSFETs, Appl. Phys. Lett. **120**, 064001 (2022).

[21] S. A. Tarasenko, A. V. Poshakinskiy, D. Simin, V. A. Soltamov, E. N. Mokhov, P. G. Baranov, V. Dyakonov, and G. V. Astakhov, Spin and optical properties of silicon vacancies in silicon carbide: A review, Phys. Status Solidi B **255**, 1700258 (2018).

[22] H. Kraus, D. Simin, C. Kasper, Y. Suda, S. Kawabata, W. Kada, T. Honda, Y. Hijikata, T. Ohshima, V. Dyakonov, and G. V. Astakhov, Three-dimensional proton beam writing of optically active coherent vacancy spins in silicon carbide, Nano Lett. **17**, 2865 (2017).

[23] http://www.srim.org/ for "SRIM: The Stopping and Range of Ions in Matter."

[24] Y. Chiba, Y. Yamazaki, S.-I. Sato, T. Makino, N. Yamada, T. Satoh, Y. Hijikata, and T. Ohshima, Enhancement of ODMR contrasts of silicon vacancy in SiC by thermal treatment, Mater. Sci. Forum **1004**, 337 (2020).

[25] T. C. Hain, F. Fuchs, V. A. Soltamov, P. G. Baranov, G. V. Astakhov, T. Hertel, and V. Dyakonov, Excitation and

recombination dynamics of vacancy-related spin centers in silicon carbide, J. Appl. Phys. **115**, 133508 (2014).

[26] Z. Wang, J. Zhang, X. Feng, and L. Xing, Microwave heating effect on diamond samples of nitrogen-vacancy centers, ACS Omega **7**, 31538 (2022).

[27] K. Hayashi, Y. Matsuzaki, T. Taniguchi, T. Shimo-Oka, I. Nakamura, S. Onoda, T. Ohshima, H. Morishita, M. Fujiwara, S. Saito, and N. Mizuochi, Optimization of Temperature Sensitivity Using the Optically Detected Magnetic-Resonance Spectrum of a Nitrogen-Vacancy Center Ensemble, Phys. Rev. Appl. **10**, 034009 (2018).

[28] J. B. S. Abraham, C. Gutgsell, D. Todorovski, S. Sperling, J. E. Epstein, B. S. Tien-Street, T. M. Sweeney, J. J. Wathen, E. A. Pogue, P. G. Brereton, T. M. McQueen, W. Frey, B. D. Clader, and R. Osiander, Nanotesla Magnetometry with the Silicon Vacancy in Silicon Carbide, Phys. Rev. Appl. **15**, 064022 (2021).

[29] H. Kraus, V. A. Soltamov, F. Fuchs, D. Simin, A. Sperlich, P. G. Baranov, G. V. Astakhov, and V. Dyakonov, Magnetic field and temperature sensing with atomic-scale spin defects in silicon carbide, Sci. Rep. **4**, 5303 (2014).

[30] X.-D. Chen, C.-H. Dong, F.-W. Sun, C.-L. Zou, J.-M. Cui, Z.-F. Han, and G.-C. Guo, Temperature dependent energy level shifts of nitrogen-vacancy centers in diamond, Appl. Phys. Lett. **99**, 161903 (2011).

[31] A. Gottscholl, M. Diez, V. Soltamov, C. Kasper, D. Krauße, A. Sperlich, M. Kianinia, C. Bradac, I. Aharonovich, and V. Dyakonov, Spin defects in hBN as promising temperature, pressure and magnetic field quantum sensors, Nat. Commun. **12**, 4480 (2021).

[32] H. Singh, M. A. Hollberg, M. Ghezellou, J. Ul-Hassan, F. Kaiser, and D. Suter, Characterization of single shallow silicon-vacancy centers in 4H-SiC, Phys. Rev. B **107**, 134117 (2023).